Radio Frequency Resonator For Continuous Monitoring Of Parallel Droplet Microfluidic Systems

D. Conchouso*[1], G. Mckerrichter[1], D. Castro[1], A. Arevalo[1], and I.G. Foulds[1,2]
[1]Computer, Electrical and Mathematical Sciences and Engineering (CEMSE), King Abdullah University of Science and Technology (KAUST)
[2]The University of British Columbia (UBC), School of Engineering, Okanagan Campus
*Corresponding author: 4700 KAUST, Kingdom of Saudi Arabia, david.conchouso@kaust.edu.sa

Abstract: This paper reports on a radio frequency sensor for the continuous monitoring of uniform droplet generation in parallel microfluidic systems. The monitoring of water in oil droplets is accomplished with the use of microwave resonators that are placed over microfluidic channels. The proposed sensor shows frequencies shifts of 50MHz for only a 5% change in water in oil content. Simulations for sensors with one and two resonators configurations are reported in here. The frequency response for the second configuration was found to be the superposition of the response of the individual resonators. This demonstrates independent frequency responses for each resonator that can be used to monitor two o more microfluidic channels without increasing the number of inputs and ouputs needed.

Keywords: RF microfluidics, Droplet Microfluidics, Droplet Monitoring, Water-Cut, Lab on Chip, Micro-strip resonator

1. Introduction

Micro-droplets are used to carry out delicate biological assays and fine chemical reactions in a confined and controlled space [1]. The inherited miniaturization associated with these nano to picoliter size droplets, creates an enhanced platform that allows reaction paths that are not possible at the macro-scale [2, 3].

Microfluidic methods offer distinct advantages over batch processes because they allow enhanced control of the overall reaction conditions (i.e. reagents mixing, temperature homogeneity, residence times, etc.) [4].

Applications for this technology can be found in the production of engineered materials such as quantum dots [5], micro & nano particles [6, 7], active pharmaceutical ingredients [8, 9], and other nano crystals [4].

Although droplet microfluidics has become an important research tool in the discovery of new materials, scale-up systems are still underdeveloped to make their way through industrial applications.

One strategy for scaling up is to parallelize hundreds of these droplet makers on a small chip [10–12]. To minimize the droplet size variability among parallel generators, different configurations have been studied [13–15].

A key characteristic that a parallel system has to maintain from the unitary one is their narrow size distribution. In other words, all generators must produce droplets of the same size in order to guarantee uniform conditions and subsequently consistent product.

The flow within channels in a parallel system is inherently coupled and undesirable clogging of one channel can lead to the failure of the entire system [10]. Therefore, continuous monitoring of the droplet dispersity is desired to prevent sources of waste or defective products.

A couple of suitable methods, to monitor the operation of parallel system, are optical inspection through image processing [16] and electrical sensing [17, 18].

Monitoring systems based on optical image processing require expensive optics (e.g. lenses, cameras, image processing units) to resolve a limited field of view, which later is analyzed and used as parameter for decision making. In a parallel system, this spacial limitation is a concern when many locations need to be monitored either within the same parallelization chip or within different

chips composing a production plant. To guarantee that the process stays within tolerances, an optical system has to either move from one location to another (i.e serial monitoring) or many optical sets are required to monitor all locations.

Electrical sensors on the other hand, can be directly integrated and manufactured within the microfluidic chip and are read straightforward. Impedance measurements [19] or radio frequency resonators [17, 20] are two candidates for the desired on-chip monitoring.

In this paper, we present a radio frequency (RF) T-resonator that can be manufactured with low cost inkjet printing technology [20]. The RF sensor detects atypical flow patterns in microfluidic channels carrying two or more fluids. In droplet microfluidics, these patterns usually occur when a droplet generator starts to malfunction due to channel clogging or fouling problems. During stable droplet generation, the resonant frequency of the T-resonator maintains a fixed value. On the other hand, if a failure occurs this frequency immediately shifts from its initial value indicating the problem.

Other applications for RF circuits in microfluidics include: measurements of the relative permittivity for different solvents [17], analysis of sugar and salt concentrations in water [21, 22] and evaluation of percentages of water in crude oil [20].

2. Device Description

A radio frequency T-resonator is comprised of an open-end transmission stub and feed lines [20, 23] that resemble a simple T-pattern. These lines are laid down on top of a microfluidic channel as shown in Figure 1 to form the sensor.

The simulated chip is made of three layers of polymethyl methacrylate (PMMA) that are bonded together to create a microfluidic channel. After bonding, the resonator lines are inkjet printed and sintered using silver ink, as described in [20]. Finally the bottom surface of the chip is covered by a metallic layer.

In droplet microfluidics there are usually two systems, either water droplets in oil (W/O) or oil droplets in water (O/W). In general, these fluids have completely different relative permittivities (Table 1) and when they are flowed together in a micro-channel, each fluid contributes towards

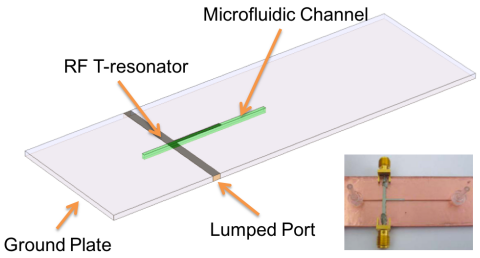

Figure 1: Microfluidic T-Resonator. The chip is formed by three layers of PMMA, the resonator lines are laid down on top of the microfluidic device, whereas the ground plate is placed on the bottom.

the complex relative permittivity of the mixture. If atypical flow is detected, the relative permittivity seen by the channel drastically changes to one of the two liquids. This change can then be measured by looking at the frequency response of the system. Typically measured as the scattering parameters (S-parameters).

The typical response for a T-resonator is shown in Figure 2. The length of the stub and effective relative permittivity of the fluid in the channel are key parameters that describe the behavior of the system.

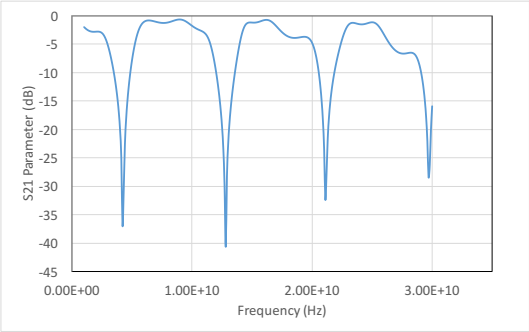

Figure 2: Frequency response for a typical T-resonator device. The system resonates at odd integers of its quarter wavelength

These microwave circuits resonate at odd integer multiples of their quarter wavelength frequency [23]. The length of the stub can be designed using the equation of a quarter wave res-

onator (Equation 1).

$$L = \frac{nc}{4f\sqrt{\varepsilon_{eff}}} \quad (1)$$

Where L is the length of the stub, n is the order of resonance ($n = 1,3,5,...$), c is the speed of light, f is the frequency and ε_{eff} is the effective permittivity.

Due to complications measuring the effective permittivity in a multi-material environment (i.e. PMMA, Oil, Water), a FEM model is often used to get an accurate solution.

3. Use of COMSOL Multiphysics

Comsol Multiphysics is used to obtain the frequency response of a simple T-resonator and to design a second microwave chip capable of monitoring two channels at the same time. This is possible if resonators with different stub lengths are placed in parallel channels and are probed by a single set of ports, as shown in Figure 3.

The idea is to design resonators that can work with as few input and output ports as possible, especially when many read outs are required like in the case of monitoring parallel microfluidic channels.

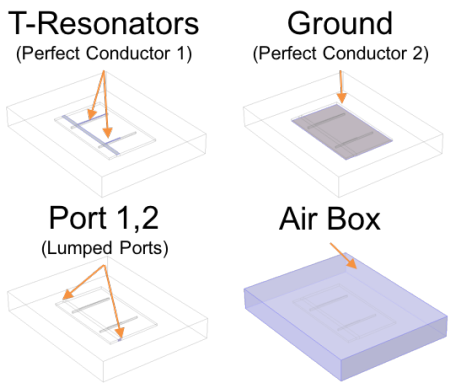

Figure 3: Double T-resonator system. Two resonators are linked together with only one feed line. Both stubs have different lengths, the longer stub is about 16*mm* whereas the shorter is 8*mm*

The electromagnetic waves, frequency domain (*emw*) interface from the radio frequency package is used to model the frequency response of the T-resonators. Source driven simulations are run for a sequence of input signals and the resonant frequencies are found plotting the s-parameters.

Material	Property	Value
PMMA	ε_r	2.7
Water	ε_r	80.4
Mineral Oil	ε_r	2.1
Copper (Cu)	$\kappa(S/m)$	$5.8x10^7$
Silver (Ag)	$\kappa(S/m)$	$2.5x10^6$

Table 1: Material properties used on the simulation

The main wave equations solved in these systems are shown below in equations 2, 3.

$$\nabla \times \mu_r^- 1(\nabla \times \mathbf{E} - k_0^2(\varepsilon_r - \frac{j\sigma}{\omega\sigma_0})\mathbf{E} = 0 \quad (2)$$

$$k_0 = \omega\sqrt{\varepsilon_0\mu_0} = \frac{\omega}{c_0} \quad (3)$$

Where μ_r is the relative permeability, ε_r is the relative permittivity, k_0 is the wave number of free space, $\mathbf{E}$ is the electric field vector

In order to evaluate the behavior of the device at high frequencies, the scattering parameters (S-parameters) relative to the electric field are measured. To achieve this, lumped ports are assigned at the resonator boundaries on both sides of the chip to approximate the connecting transmission lines.

The s-parameters are calculated in COMSOL performing an eigenmode expansion of the electromagnetic fields on the ports. The fields are assumed to be normalized with respect to the power flow across each port.

The computed electric field E_c is given by equation 4.

$$S_{21} = \frac{\int_{port2}(\mathbf{E_c} \cdot \mathbf{E_2^*})dA_2}{\int_{port2}(\mathbf{E_2} \cdot \mathbf{E_2^*})dA_2} \quad (4)$$

For convenience, this transmitted power is also defined on a dB scale using equation 5.

$$S_{21dB} = 20log_{10}(|S_{21}|) \quad (5)$$

For the sake of the present simulation, the material properties of the resonator and fluids are summarized in Table1.

4. Simulation Results and Discussion

The response of a single droplet generator when the channel is filled with a fluid is presented in Figure 4. In this plot, we evaluated the power transmitted from Port 1 to Port 2 (S_{21}) in order to characterize the behavior of the system for a range of different permittivities varying from pure water to pure oil.

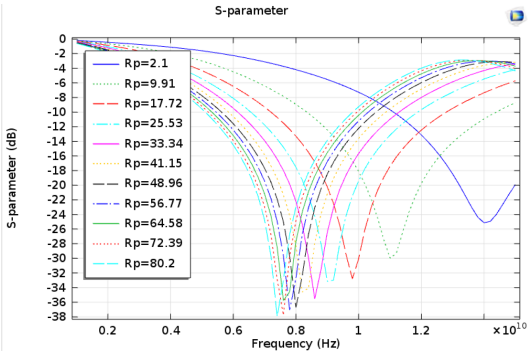

Figure 4: S_{21}-Parameter for fluids with relative permittivities ranging from pure water ($\varepsilon_r = 80.2$) to pure oil ($\varepsilon_r = 2.1$). Note: *Rp* in the legend denotes relative permittivity

At permittivities closer to water, the fundamental frequency decreases. Whereas, at permittivities closer to oil the resonant frequency increases. This shift can then be used to detect atypical flow behavior in channels containing droplets in a carrier fluid. A change as low as 5% in the concentration of water, produced up to 50MHz shift in the resonant frequency of the device.

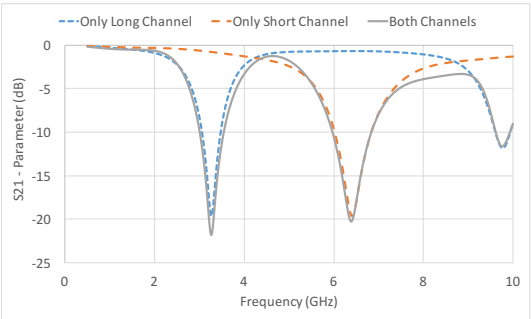

Figure 5: Superposition of the frequency responses for a double T-resonator system. (The denoted long channel is 16*mm* whereas the short channel measures only 8*mm*)

In the case of the device depicted on Figure 3, stubs with lengths of 16mm and 8mm were chosen for this study.

The frequency response for each individual stub was calculated in order to avoid undesirable interference between resonators. First, the shorter stub was removed from the model and only the frequency response for the long stub was obtained. Then the response of only the short stub was also calculated.

A comparison was made between the sum of the frequency responses of each stub with the response of double T-resonator system, as shown in Figure 5. The response shows accurate superposition with very minimal coupling effect between both resonators. Since there are no interferences with other modes of resonance, these two parallel resonators can react independently to detect effective permittivity changes due to atypical fluid flow. This systems requires only one input/output to monitor two channels at the same time.

5. Conclusions

RF sensing is a promising approach for monitoring parallel microfluidic channels carrying microdroplets. The micro-strip T-resonator, proposed in this paper, shifts its resonant frequency by 50MHz when the water in oil concentration changes as low as 5% for W/O systems.

This technology can be integrated to current microfluidic chips and requires of fewer number of probes than an impedance measurement.

Although the parallel RF sensor works accurately with two resonators, the number of resonators that can be put together cannot be expanded to many because each resonator needs a finite bandwidth to operate independently.

The COMSOL simulations allowed us to get a better understanding of the system and to quickly vary key elements of design such as the effective permittivities of the fluids and substrate, stub length, and distance between resonators.

6. References

1. A B Theberge, Fabienne Courtois, Yolanda Schaerli, Martin Fischlechner, Chris Abell, Florian Hollfelder, and Wilhelm T S Huck. Microdroplets in Microfluidics: An Evolving Platform for Discoveries in Chemestry and Biology. *Small*, **49**:5846–5868 (2010).

2. Marie Leman, Faris Abouakil, Andrew D Griffiths, and Patrick Tabeling. Droplet-based microfluidics at the femtolitre scale. *Lab on a Chip*, **15**(3):753–765, (2015).

3. P Gravesen, J Branebjerg, and O S Jensen. Microfluidics-a review. *Journal of Micromechanics and Microengineering*, **3**(4):168–182 (1999).

4. Thomas W Phillips, Ioannis G Lignos, Richard M Maceiczyk, Andrew J deMello, and John C deMello. Nanocrystal synthesis in microfluidic reactors: where next? *Lab on a Chip*, **14**(17):3172–3180 (2014).

5. Adrian M Nightingale and John C de Mello. Controlled Synthesis of III-V Quantum Dots in Microfluidic Reactors. *ChemPhysChem*, **10**(15):2612–2614 (2009).

6. EM Chan, AP Alivisatos, and RA Mathies. High-temperature microfluidic synthesis of CdSe nanocrystals in nanoliter droplets. *Journal of the American Chemical Society*, **127**(40):13854–13861, (2005).

7. Suhanya Duraiswamy and Saif A Khan. Droplet-Based Microfluidic Synthesis of Anisotropic Metal Nanocrystals. *Small*, **5**(24):2828–2834, (2009).

8. Arpad I Toldy, Abu Zayed M Badruddoza, Lu Zheng, T. Alan Hatton, Rudiyanto Gunawan, Raj Rajagopalan, and Saif A Khan. Spherical crystallization of glycine from monodisperse microfluidic emulsions. *Crystal growth & design*, **12**(8):3977–3982, (2012).

9. Reno AL Leon, Wai Yew Wan, Abu Zayed M Badruddoza, T. Alan Hatton, and Saif A Khan. Simultaneous spherical crystallization and co-formulation of drug (s) and excipient from microfluidic double emulsions. *Crystal growth & design*, **14**(1):140–146, (2013).

10. D. Conchouso, D. Castro, S. A. Khan, and I. G. Foulds. Three-dimensional parallelization of microfluidic droplet generators for a litre per hour volume production of single emulsions. *Lab on a Chip*, **14**(16):3011–3020, (2014).

11. Takasi Nisisako, Takuya Ando, and Takeshi Hatsuzawa. High-volume production of single and compound emulsions in a microfluidic parallelization arrangement coupled with coaxial annular world-to-chip interfaces. *Lab on a Chip*, **12**(18):3426–3435, (2012).

12. Goran T Vladisavljević, Nauman Khalid, Marcos A Neves, Takashi Kuroiwa, Mitsutoshi Nakajima, Kunihiko Uemura, Sosaku Ichikawa, and Isao Kobayashi. Industrial lab-on-a-chip: Design, applications and scale-up for drug discovery and delivery. *Advanced Drug Delivery Reviews*, **65**(11-12):1626–1663 (2013).

13. D. Conchouso, E. Al Rawashdeh, A. Arevalo, D. Castro, and I. G. Foulds. Simulation of a 3D Flow-Focusing Capillary-Based Droplet Generator. In *COMSOL Conference, Rotterdam, Netherlands.*, (2013).

14. D. Conchouso, E. Rawashdeh, D. Castro, A. Arevalo, and I. G. Foulds. Optimized Channel Geometry of a Flow-Focusing Droplet Generator for Parallelization. In *Proceedings of the 2013 COMSOL Conference*, Rotterdam (2013).

15. D. Conchouso, A. Arevalo, D. Castro, Y. Yi, and I. G. Foulds. Simulation of Constant-Volume Droplet Generators for Parallelization Purposes. In *COMSOL Conference, Grenoble, France*, (2015).

16. Amar S Basu. Droplet morphometry and velocimetry (DMV): a video processing software for time-resolved, label-free tracking of droplet parameters. *Lab on a Chip*, **13**(10):1892–1901, (2013).

17. Ali A Abduljabar, David J Rowe, Adrian Porch, and David A Barrow. Novel Microwave Microfluidic Sensor Using a Microstrip Split-Ring Resonator. *IEEE Transactions on Microwave Theory and Techniques*, **62**(3):679–688, (2014).

18. Caglar Elbuken, Tomasz Glawdel, Danny Chan, and Carolyn L Ren. Detection of microdroplet size and speed using capacitive sensors. *Sensors and Actuators A: Physical*, **171**(2):55–62 (2011).

19. Tao Sun and Hywel Morgan. Single-cell microfluidic impedance cytometry: a review. *Microfluidics and Nanofluidics*, **8**(4):423–443 (2010).

20. G. McKerricher, D. Conchouso, B. S. Cook, I. G. Foulds, and A. Shamim. Crude oil watercut sensing with disposable laser ablated and inkjet printed RF microfluidics. In *Microwave Symposium (IMS), 2014 IEEE MTT-S International IS - SN - VO* -, pages 1–3, I, (2014).

21. H Zhang. Dual-band Microwave Components and Their Applications. (2011).

22. S Pinon, D L Diedhiou, A Boukabache, V Conedera, D Bourrier, A-M Gue, G Prigent, E Rius, C Quendo, B Potelon, and J-F Favennec. Fabrication and characterization of a fully integrated biosensor associating microfluidic device and RF circuit. *Microwave Symposium Digest (MTT), 2012 IEEE MTT-S International*, pages 1–3, (2012).

23. K P Latti, M Kettunen, J P Strom, and P Silventoinen. A Review of Microstrip T-Resonator Method in Determining the Dielectric Properties of Printed Circuit Board Materials. *Instrumentation and Measurement, IEEE Transactions on*, **56**(5):1845–1850, (2007).